Modelling of Arc Faults in 48 V Automotive Power Supply Systems

Michael Kiffmeier, Selcuk Önal, Carina Austermann, Stephan Frei
TU Dortmund University
Dortmund, Germany
michael.kiffmeier@tu-dortmund.de

***Abstract* — As a new voltage level, 48 V has been introduced to automotive power supply systems. As a consequence, new critical phenomena, arcs, may arise. These arcs can cause serious damages, even fire. In this paper, arcs in 48 V automotive power supply systems are investigated and a full model is developed and parameterised. Electrical models are required to clarify the connection between the arc characteristics and the power net components itself. Conditions promoting arcs and inhibiting arcs can be developed. Model based arc detection strategies demand for accurate models, too. Transient phenomena as well as operation points are considered. Additionally thermal investigations of arcs are carried out to evaluate the severity of different arcs. Methods for burn time prediction based on dissipation power of arcs are presented.**

Keywords—48 V; Automotive Power Supply System; Arc;

I. INTRODUCTION

Through the progressive electrification and special requirements from autonomous driving systems, more and more electronic control systems (ECU) take place in the established 12 V power nets. Some of the newly integrated systems have a quite high power demand, and several of the established consumers increase their power demands, too. To lower the necessary currents, a new voltage level has been introduced and implemented – 48 V.

Beside the known 12 V faults in energy supply systems, in 48 V power nets a new kind of fault may occur: arcs. In this paper, an arc model approach is presented. This model considers the characteristic phases of the arc phenomenon. These phases will be explained, taking the actual power net into account. Based on the developed model, different system combinations can be evaluated with regard to the ability of arcs to reach a steady state, or burn for a critical time, resulting in a critical amount of energy to be dissipated. If so, the energy can be used to estimate the thermic behaviour of an arc. With this information, it is possible to assess the risk of material damage or fire.

II. SPECIAL AUTOMOTIVE REQUIREMENTS FOR ARC MODELS AND MODELLING APPROACHES

A. Series and Parallel Arcs in 48 V Power Supply Systems

An example for a simple vehicle power net is depicted in Fig. 1.

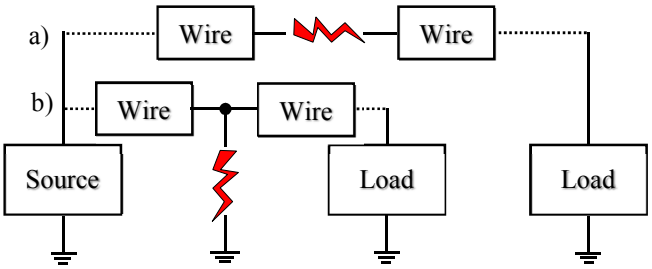

Fig. 1. Scheme of a power net with a) series arc fault and b) parallel arc fault.

The basic classification of arcs in supply systems can be seen. On the one hand, loose connections and opening connectors can lead to series arcs. On the other hand, short circuits to ground can let parallel arcs occur. Arcs might not necessarily bring a system in a malfunction state, thus detection might be difficult. In general, series and parallel arcs are very similar in nature. Research on both can be done on the basis of the given model.

B. Known DC low-voltage arc modells

Over the years, the problem of arcs in DC power supply systems has already come up in several different fields. Many DC arc models have already been developed, e.g. [1] [2] [3]. These models always cover some specific requirements, e.g. materials, voltage range or current range and cannot be applied directly to automotive 48 V. Furthermore, to investigate the ignition and burn behaviour the environment has to be taken into account. For this reason, this paper focuses on a circuit representation of an arc, so that it can be implemented in already existing system simulations. Basically, DC arcs can be described with various circuits. Some, for 48 V suitable, available models that support the observed arc behaviour are discussed and extended.

The great majority of the existing arc models are derived from the V-I-characteristics and can reflect only specific operation points of arcs, depending on a chosen input circuitry and electrode distance [4]. This behaviour can be modelled by an equivalent voltage source. The voltage drop can be divided into three parts. An instantaneous arising, strongly material dependent, voltage step v'_{ac}, a linear, mainly length dependent voltage drop $E \cdot d$, and a nonlinear, current and length dependent voltage drop $f(d, i_{arc})$. This is outlined e.g. in the Ayrton Equation [5].

$$v_{arc} = v'_{ac} + E \cdot d + f(i_{arc}, d) \tag{1}$$

The gradient E represents the linear dependency [6], the last term shows the nonlinear connection between v_{arc} and i_{arc}. The resulting distance and length dependent part of the voltage drop is also called column voltage drop v_{col}, the overall resulting instantaneously rising voltage drop anode cathode voltage drop v_{ac}, which may depend on parameters chosen for the representation of $f(i_{arc}, d)$. Several other arc voltage equations lead to similar principles, such as the Steinmetz Equation [7] or Nottingham Equation [8]. Taking the burn conditions v_{min} and i_{min}, derived from the V-I-diagram, into account, with regard to an equivalent circuit representation, a variable resistor can be added, like in [2].

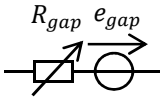

Fig. 2. Arc model approach using a nonlinear resistor and a voltage source.

The resistor can be used to produce the specific behaviour in the extinction moment. In this moment, the equivalent voltage source will disappear, $e_{gap} = 0$ and R_{gap} will rise to a high value, representing an open circuit. Beneath the above mentioned burn conditions, another reason for the expiration can be pointed out. At a critical electrode distance the arc will expire, too.

The described model principles are used in the following to investigate and explain the arc behaviour in a typical automotive power supply system environment. These investigations have been performed for static and transient phenomena.

III. Arc Measurements and Modelling Approach for the use in 48 V Power Supply Systems

For being able to perform arc investigations, an appropriate test bench has been built to perform arc events in a simplified automotive power supply system. The power supply system, that has been considered, is presented in Fig. 3. A control unit, modeled by a stability capacitor and an ohmic load, such as heating elements, has been chosen as common load configuration.

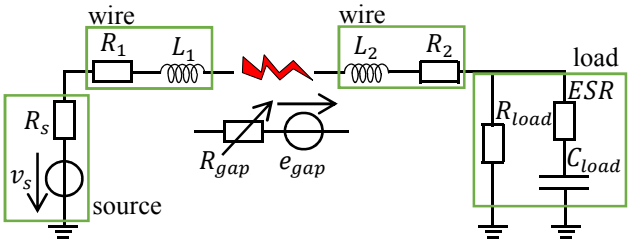

Fig. 3. Considered system model. Component models that consider dynamic behaviour, as well, are used to simulate the entire system behaviour of the simplified 48 V automotive power supply system, depicted in Fig. 1.

Several test series have been performed with typical automotive plug-in contacts. Thus, the material of the electrodes was tinned brass. The test bench was built with a stepper motor and a rotating shaft. With this setup, tests have shown a very high precision. A satisfying reproducibility could be proved, as well. The test bench is shown in Fig. 4.

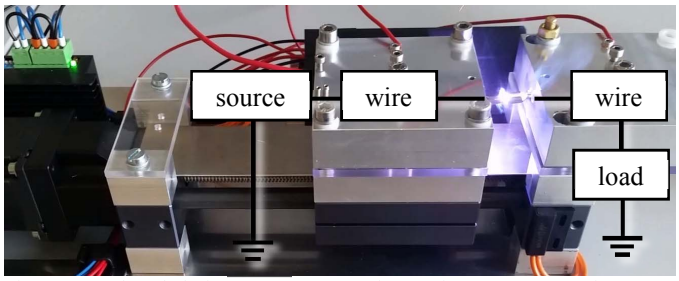

Fig. 4. Test bench during an arc event. Series Arc in a 48 V automotive power supply system with 8 A nominal current.

Fig. 5 shows characteristic voltage signatures of a typical arc behaviour within the above mentioned circuit. In both cases the electrodes have been separated with a constant speed of $7.55\ mm/s$ until the arc expires. On the left, the load does not have a capacitive component. On the right, a capacitive component has a significant impact on the event.

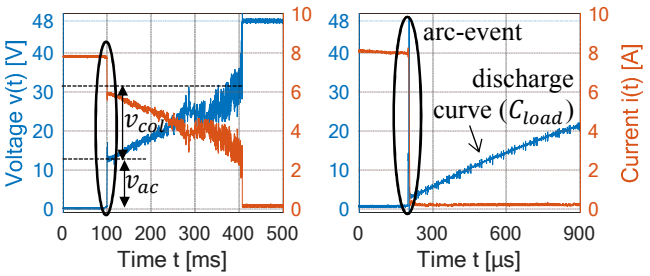

Fig. 5. Voltage and current profiles of series arc in the described setup; left: arc event until maximum arc length is reached; right: arc event expires right after ignition; Zoomed in Fig. 6;

On the left, a change of operating points due to the increase of the electrode distance can be seen. There is a clear difference between the instantaneous voltage step v_{ac} in the ignition moment and the length dependent voltage drop v_{col}. On the right, the ignition phase is interrupted and after the arc extinction, the discharge curve due to C_{load} can be measured. The circled areas are presented in a higher resolution in Fig. 6.

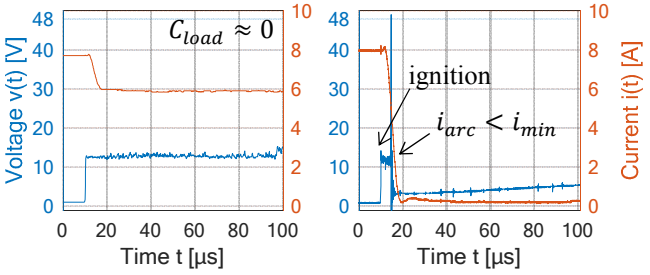

Fig. 6. Zoomed areas from Fig. 5; left: Ignition process not interrupted; right: ignition interrupted;

A small displacement between voltage and current may has happened because of the different bandwidths of the probes.

IV. DETAILED DESCRIPTION OF ARC PHASES DURING THE EXISTENCE TIME

The arc event can be separated into several phases, e.g. [9]. These phases are described, analysed and modelled in the following.

A. *Molten bridge (before arc)*

Once the electrodes are being separated, the contact area becomes smaller, and in consequence, the current density increases permanently. At some point, the current density is high enough to melt the material and create a so called molten bridge [9]. This molten bridge already shows a reduced conductivity and causes a small voltage drop of about up to $2\ V$. Due to the very short existence and only weak influence on the system, this state has not been considered in the further modelling effort.

B. *Transient response in the high slope voltage raising moment (arc ignition phase)*

The next phase in the arc ignition moment is a very steep voltage step. The slope can have values up to $5 \cdot 10^9\ V/s$ [9]. Especially in this moment, the dynamic properties of the entire circuit can have a significant effect on the arc itself. The arising transient phenomenon can be represented by taking the arc's anode and cathode voltage drop v_{ac} into account. This means, as model simplification, a step switching voltage source can be used. The steep voltage step creates oscillation in the arc current, due to the wire inductors and the load capacitor, which also may behave like the aperiodic sequence. As soon as the oscillation brings the current below a limit i_{min}, the arc ignition is interrupted. In this case, the arc model changes to a resistive behaviour with a fast increasing high resistance, representing the resulting gap, and opening the circuit.

If the oscillating current stays above a minimum current, the process of arc ignition can be completed and the arc reaches a steady state. Both cases are presented and the modelling approach is validated in Fig. 7.

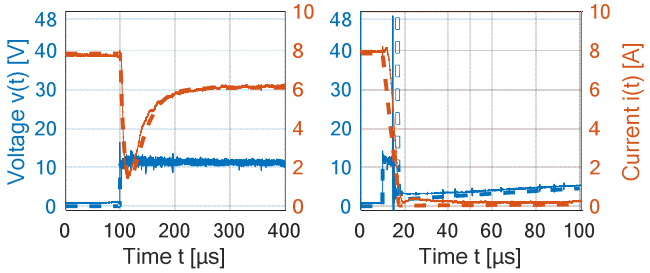

Fig. 7. Voltage and current signature of series arcs – dashed: simulation ($v_B = 48\ V, R_B = R_1 = R_2 = 5\ m\Omega, L_1 = L_2 = 5\ \mu H, R_{load} = 6.1\ \Omega$) ; left: oscillation (aperiodic borderline case), but still above i_{min} ($C_{load} = 20\ \mu F, ESR = 1650\ m\Omega$); right: arc interruption in ignition moment ($C_{load} = 200\ \mu F, ESR = 500\ m\Omega$); $v_{min} = 10.8\ V, i_{min} = 1\ A$ (can be lower during the ignition process);

With these assumptions, limits and modelling effort, the conditions for an arc ignition can be evaluated, depending on the circuit properties and components. For a given wire length, respectively a constant value for L_1 and L_2, the evaluation can be found in Fig. 8 (right).

However, not only the RLC oscillating circuit in combination with the i_{min} current condition can deliver an explanation for the described behaviour. In the moment of ignition, the inductive parts within the circuit (L_1 and L_2 in the model) produce induced voltages. These voltages can keep the arc alive as long as the source voltage is still bound in the capacitor. If the capacitor discharge is not fast enough, the short voltage peak, caused by the inductors decays before the minimum voltage v_{min} has been released by the capacitor. Supervising this criteria is not practical in the simulation due to the arc representation as a controlled voltage source.

In general, arcs do have a partially chaotic and random nature. Even if the arc has already expired due to the mentioned events, a re-ignition is still possible. In this context, a direct connection with the described time constant of the RC-circuit (load) can be found. As soon as the necessary voltage v_{min} can be provided after the expiration, the re-ignition can take place. On the one hand, this may be due to real mechanical conditions, such as vibrations, or a rough surface. Another explanation for this behaviour can be gathered by a probabilistic approach. Similar to ESD-pulses, a statistical time lag can model the re-ignition [10]. Thus, the re-ignition takes place with a decreasing probability over time.

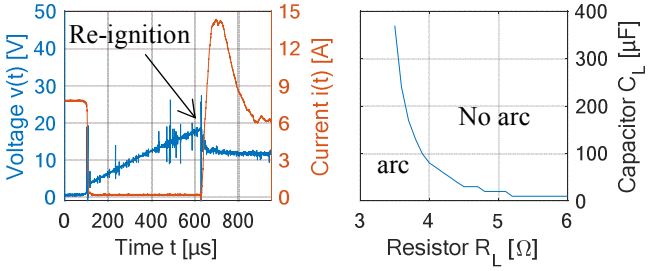

Fig. 8. Left: voltage and current signature in the occurrence of a re-ignition; right: evaluation of the arc ability to reach a steady state based on the presented model without taking reignition into account ($ESR = 1\ \Omega, L_1 = L_2 = 5\ \mu H$);

C. *Steady-state behaviour (arc in operation points)*

After the arc has reached a steady state, not only the anode and cathode voltage drop has to be taken into account, but also the length dependent column voltage drop in addition to the nonlinear part caused by i_{arc}. This means, a variable voltage source can be used, with basically $v = f(i_{arc}, d)$, as described in the beginning (1). For parameterising the needed parameters, such as the gradient, several measurements in different operating points have been performed. During the measurements, the first point of arc occurrence is detected by the test bench controller. From this point, the tuned moving-profiles can be applied. The electrode distance has been tuned precisely in a typical range $d = 0 \ldots 1.25\ mm$, the values for the nominal current i_n have been varied between values close to the minimum current limit for arcs and $i_{n,max} \approx 15\ A$. The results can be found in Fig. 9.

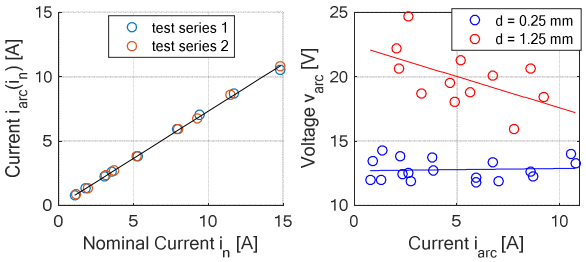

Fig. 9. Left: dependency between the nominal current and the current in an arc event ($d = const. = 0.25\ mm$); right: Dependencies between v_{arc}, i_{arc} and d, incl. interpolation models;

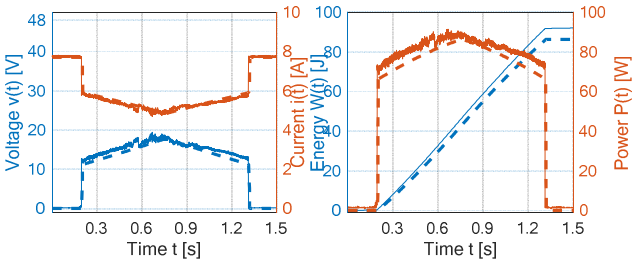

Fig. 10. Comparison of arc measurement and arc simulation; left: arc current and arc voltage; right: arc power and arc energy ($v_B = 48\ V, R_B = R_1 = R_2 = 5\ m\Omega, L_1 = L_2 = 5\ \mu H, R_{load} = 6.2\ \Omega$)

This phase of the arc event can be modelled by using the voltage source again, in addition with the length and current dependent voltage drop.

D. *Model parameterisation*

A summary of the before mentioned phases can lead to an arc model. The parameters are obtained by measurements in the described circuit for the operation points, found in Fig. 9 (left).

The resulting equation depends on the assumptions for the last term $f(d, i_{arc})$. Taking a multiple linear regression approach into account, which can give good results for interpolation, the following parameters occur:

$$v_{arc} = 10.3\ V + 9.7\ \frac{V}{mm} \cdot d + 0.14\ \Omega \cdot i_{arc} - 0.5\ \frac{V}{mm\ A} \cdot d \cdot i_{arc} \quad (2)$$

On the other hand, an extrapolation can be achieved better by fulfilling the nonlinear requirement.

$$v_{arc} = 11.6\ V + 4.7\ \frac{V}{mm} \cdot d + \frac{9.9\ \frac{VA}{mm} \cdot d - 2.5\ VA}{i_{arc}} \quad (3)$$

These parameters fulfil the requirements for the presented measurements, but may vary in different setups and environments. Another important information can be given for the parameters used in (2) and (3). The selected equation is valid to model the arc behaviour in various operating points, represented by different arc lengths. This can be seen in Fig. 10. Here equation (3) was used and the electrode distance, respectively the plug distance, has been precisely varied from contact ($d = 0\ mm$) to $d = 1\ mm$, then back to contact. So, the voltage drop increases until the maximum distance has been reached, and diminishes again when the moving direction was inverted. This moving profile can be used in order to imitate a loose plug.

However, throughout this paper, different phases have been described with the help of model simplifications. The activation function of the above mentioned equation can be given by $\tanh(\lambda \cdot t_{arc})$, with t_{arc} as the arc existing time and λ for being able to tune the average slope. This activation must be 0 for $t_{arc} < 0$. To take off the voltage source's influence in the moment of extinction, a similar, substracting deactivation function can be used. Approaches for the transitions between the different phases are presented in a similar way compared to [2]. Also in the extinction moment, the resistive behaviour of the arc has to increase until the arc voltage reaches the source/maximum available voltage. In [2] this has been reached by controlling R_{gap} so that it has a voltage drop equal to the source voltage (v_s/i_{arc}), with an additional weight term. This term has an exponential rise until the arc voltage drop equals the source voltage. However, another way for keeping a similar behaviour, without taking the source into account, is to create the resistive behaviour of the arc with an exponential rise of the form $R_{off} \cdot \exp(\alpha \cdot (t_{exp} - T_{exp}))$, with R_{off} as open circuit resistance, t_{exp} as timer for the expiration phase, starting with 0 in the expiration phase, and T_{exp} as time for expiration. α can be used to tune the resistive influence during the arc event. The reach of a critical distance or the falling below the minimum current must turn the model into this phase. To prevent a voltage collapse in the extinction moment, R_{gap} must be valued in the extinction moment so that the arc voltage keeps constant (v_{arc}/i_{arc}).

V. Thermal Investigation on Arcs in 48 V Power Supply Systems

During an arc event, a high power dissipation can be obtained, so the resulting high temperatures can ignite various materials, such as sleevings or contact housing, in its vicinity. In Fig. 11 the time dependent power loss in a plug contact during an arc event is shown (blue), the measured temperature is given, as well (red). In order to ensure a homogenous known surface emissivity, graphite spray was used for thermal imaging. To avoid a change in electrical behaviour of the electrodes the coating was omitted for the switching contact parts. The real temperature for parts close to the arc are assumed to be much higher because of the decreased surface emissivity.

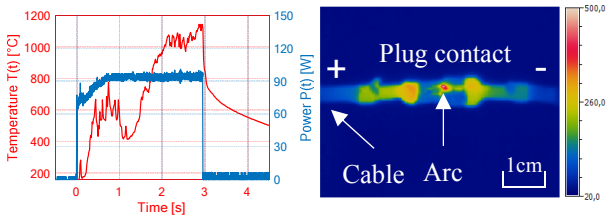

Fig. 11. Power and temperature for a contact during low power arcing (left); IR measurement (right)

Based on the energy conservation law, the energy balance equation for an arc between two electrodes of an electrical contact can be set up as follows.

$$P_{arc} = P_{conv} + P_{rad} + P_{cond,rad} + P_{cond,ax} \qquad (4)$$

Here P_{arc} represents the measured electrical dissipation power of the arc, P_{rad} the power dissipated by radiation, P_{conv} by convection, $P_{cond,rad}$ by radial conduction and $P_{cond,ax}$ is the power dissipated by axial heat conduction into the electrodes and cables.

A. *Ignition times of surrounding insulation materials*

Due to the complex nature of arcs it is very difficult to calculate the exact ignition times of insulation materials that are not in direct contact with the arcing electrodes. However, it is possible to investigate the relationship between arc power and ignition times for specific insulating materials using absorbed radiative power density and their ignition rates [11]. So, Fig. 12 shows the estimated times to ignition as a function of absorbed power density for various materials [11].

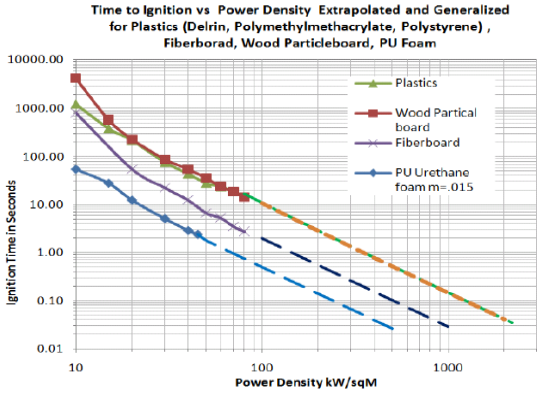

Fig. 12. Ignition time vs. arc power density generalised for plastics [11]

As a worst-case scenario, it can be assumed that the whole electrical power generated by the arc is dissipated by radiation. With this assumption, it becomes possible to calculate the time to ignition for a specific insulation material that surrounds the electrical arc. To estimate the total absorbed radiative power the view factor, depending on the geometry, has to be estimated. Fig. 13 illustrates the configuration that can be used to describe the setup: An arc is surrounded by an insulation material in a certain distance. Here, the arc can be represented by a thermal isotropic radiator, whereas the insulation surface is considered to be a cylinder. Only the closest points, respectively the highest power density points, are considered for the calculation of the time to ignition.

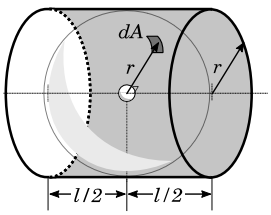

$$F_{1-2} = \frac{1}{\sqrt{1+\left(\frac{r}{l/2}\right)^2}}$$

Fig. 13. Description of considered geometrie, the arc is represented by a thermal isotropic radiator (left); corresponding view factor, which can be used to calculate the total absorbed power (right) [12]

The highest radiative power density on the surface of the insulation (surface A) can be used to determine the time to ignition. This is a crucial factor and is calculated with the equation:

$$P'_{abs,max} = \frac{P_{arc}}{4\pi r^2} \qquad (5)$$

Combining the mentioned observations and the data from Fig. 12, the time to ignition can be provided. Fig. 14 shows the times to ignition caused by an arc with varying dissipation power with different values of the distance between the arc and the insulation material.

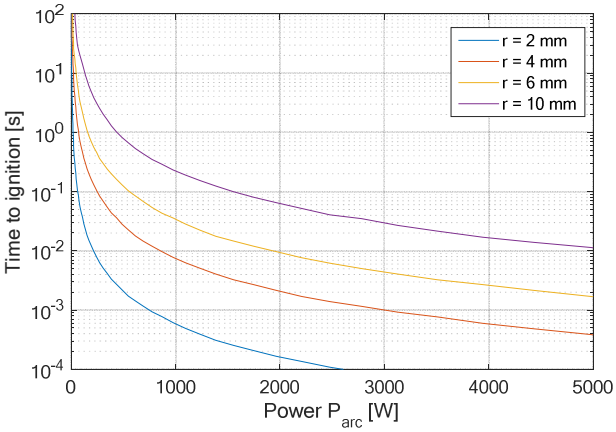

Fig. 14. Time to ignition vs. arc power P_{arc} for different distances between the arc and the insulation material

B. *Example application of thermal approaches*

The resulting dissipation power of arcs highly depends both on the entire power network and on the relative position to the power net components, means parallel or series arc. It can be in a wide range of e.g. a few hundred watts or even less (see Fig. 11), up to the kilowatts area, which can be typically found for parallel arcs or series arcs in high current branches. The detection and handling of an arc fault within a 48 V automotive power supply systems is absolutely necessary. To define requirements for a diagnosis algorithm, especially for the maximum time needed to detect and handle the fault, the above shown diagrams can be used.

As an example, Fig. 11 shows a 90 W arc that exists for around 3 seconds. If an insulation material was placed around the arc with a distance of 4 mm, it would have ignited after around

600 ms, in the described worst case situation. So, for the circuit under investigation, to avoid a serious damage, arcs are only allowed to hold for maximum 600 ms.

C. Lumped Parameter Model for estimating of ignition times

The curves in Fig. 14 can also be approached by means of a thermal equivalent RC-Network, e.g. Foster-Network (see Fig. 15), whose parameters can be extracted by curve-fitting considering a critical temperature. With the help of this thermal network the time to ignition can be estimated for an arc power which doesn't have a constant profile.

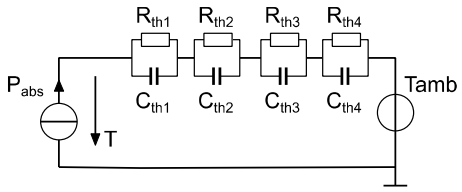

Fig. 15. Equivalent thermal network: Foster-Network for electrical simulation of thermal processes;

Considering the joule heating, performed solely by the arc, P_{abs} will be $P_{arc} \cdot F_{1-2}$ and T_{amb} represents the absolute ambient temperature. This model also allows to estimate a temperature T, which can be assumed to be the critical igniting temperature of an insulating surface. In particular, this is expected to be a constant value in contrast to a critical arc temperature.

VI. CONCLUSION

In this paper, the arc phenomena during the entire arc event have been analysed and modelled. The developed modelling approach is easy to use and can be integrated in electric network based simulations of entire complex power nets. It is based on measurements, made under typical boundary conditions that can be found in cars environments. Care must be taken as the behaviour of arcs is always a statistical process with many uncertainties. From the developed electrical model, dissipation power predictions were used to make a statement regarding to the thermal behaviour of the arc, as well. So, e.g. requirements for arc detection algorithms can be derived.

ACKNOWLEDGMENT

The author would like to thank the German Federal Ministry for Economic Affairs and Energy for funding the research project DriveBattery 2015 (grant number 03ET6060H). The responsibility for this publication rests solely with the author.

REFERENCES

[1] R. F. Ammermann, T. Gammon, P. K. Sen and J. P. Nelson, "DC-Arc Models and Incident-Energy Calculations," IEEE Transactions on Industry Applications, VOL.46, NO.5, September/October 2010.

[2] F. M. Uriarte, A. L. Gattozzi, J. D. Herbst, H. B. Estes, T. J. Hotz, A. Kwasinski and R. E. Hebner, "A DC Arc Model for Series Faults in Low Voltage Microgrids," IEEE Transactions on smart grid, VOL.3, NO.4, December 2012.

[3] F. M. Uriarte, H. B. Estes, T. J. Hotz, A. L. Gattozzi, J. D. Herbst, A. Kwasinski and R. E. Hebner, "Development of a Series Fault Model for DC Microgrids," IEEE PES Innovative Smart Grid Technologies, 2011.

[4] A. N.-B. Wu, "Investigation of Electric Arcs in 42 Volt Automotive Systems," Massachusetts Institute of Technology, 2001.

[5] H. Ayrton, The Electric Arc, London: The Electrician, 1902.

[6] W. Rieder, Plasma und Lichtbogen, Braunschweig: Friedr. Vieweg & Sohn GmbH, 1967.

[7] C. P. Steinmetz, "Transformation of electric power into light," American Institute of Electrical Engineers, New York, 1906.

[8] W. B. Nottingham, "A New Equation for the Static Characteristic of the Normal Electric Arc," American Institute of Electrical Engineers, New York, 1925.

[9] R. Haug, T. Kouakou and J. Doremieux, "Phenomena preceding arc ignition between opening contacts: experimental study and theoretical approach," Electrical Contacts, IEEE, Montreal, Quebec, Canada, 1990.

[10] S. Frei, M. Senghaas, R. Jobava and W. Kalkner, "The Influence of Speed of Approach and Humidity on the Intensity of ESD," International Zurich Symposium, Zurich, 1999.

[11] J. K. Hastings, M. A. Juds, C. J. Luebke and B. Pahl, "A study of ignition time for materials expsed to dc arcing in PV systems," 37th PVSC, Washington, 2011.

[12] M. F. Modest, Radiative Heat Transfer; Third Edition, USA: Academic Press is an imprint of Elsevier, 2013.

[13] K. Singhal and J. Vlach, Computer Methods for Circuit Analysis and Design, Van nostrand Reinhold Electrical/Computer Science and Engineering Series, 1983.

[14] V. Degardin, L. Kone, F. Valensi, P. Laly, M. Lienard and P. Degauque, "Characterization of the High-Frequency Conducted Electromagnetic noise Generated by an Arc Tracking Between DC wires," IEEE Transactions on Electromagnetic Compatibility, 2016.

[15] P. Slade, Electrical Contacts: Principles and Applications, Florida: CRC Press, 2014.